Data-Driven Ice Blockage Estimation of Water Intake at Niagara Hydropower Station

Koji Yamashita and Nanpeng Yu

Electrical and Computer Engineering
University of California Riverside
Riverside, CA, USA

Qing Wei

Research, Technology Development & Innovation
New York Power Authority
White Plains, NY, USA

***Abstract*—Frazil ice and anchor ice could cause ice blockage at water intakes, which results in shutting down intake facilities and/or lowering the active power output of the hydropower plant. This paper proposes a data-driven ice blockage estimation method for the water intake. Specifically, the flow velocity coefficient of the conduit is calculated from water levels at the water intake and forebay, and water flows at hydropower units in conjunction with the water storage and leveraged as the index for ice blockage. Detection conditions and rejection conditions are showcased to extract only highly probable ice blockage events and exclude false positives, respectively. The ice blockage estimation performance was examined with eleven years of historical data at Niagara hydropower stations. System operation logs demonstrate that the anchor ice, lake ice, and shore ice were continuously observed 4-15 hours before the three detected occurrences, which serve as evidence of the validity of the proposed method.**

***Index Terms*—Anchor ice, frazil ice, hydropower plant, ice blockage, water intake.**

I. Introduction

On the river and lake, specifically the frazil ice and anchor ice, are one of the significant concerns pertaining to the hydropower generation operation. Such ice in the frozen river may eventually lead to obstructed intake, which results in a huge loss of generation (e.g., shutting down the intake facility [1] or lowering the active power output target to the minimum level [2]). This event is known as the ice blockage at the water intake [3]. This is not a new phenomenon, as a complete blockage of the water intake occurred in Russia in 1914 due to the frazil ice. Similar events in the 21st century are reported at Lake Michigan in 2003 [2], the St. Lawrence River in 2005-2006 [4], and the Mille-Iles River in 2020-2021 [5].

The frazil ice would generally glue itself to the underside of the floating river ice. Especially when the river ice gets stuck, the frazil ice could grow downward, which increases the risk of ice blockage at the water intake. On the other hand, the anchor ice generally grows at the bottom of the river, and it could glue to stones in the riverbed. In particular, if the anchor ice removes those stones, it flows towards the intake with those stones, which can cause the risk of obstruction at the intake.

The ice formation, evolution, and characteristics have been well studied [6]–[8], and many researchers have focused on the early awareness/discovery of the frazil ice and anchor ice [9]. The countermeasure of the ice blockage, mostly the heater, is also discussed in some scholarly articles [10]. However, how the ice blockage at the water intake affects the hydropower system is not studied as thoroughly. The reference [2] only details the impact of the ice blockage at the water intake. First, the forebay elevation (or water level) decreases around an hour after the frazil ice starts to formulate. Second, the water flow decreases a few hours after the ice formation. The authors in [2] interpret the above impact as the increase in the head loss. Then they propose to monitor and track the ice blockage at the water intake using two indices: the water level drop at the forebay and the head loss level rise between the intake and the forebay.

In this paper, we propose to use the flow velocity coefficient of the conduit instead of the head loss to monitor and detect the state change caused by the ice blockage at the water intake. We leveraged eleven years of historical data in the range of 2011 and 2021 at the Niagara River for quantifying the performance of this proposed approach. Screening procedures are created and applied to the proposed ice blockage estimation approach mainly for coping with the false positive, i.e., output the ice issue flags in spite of no ice blockage occurrence.

The organization of the paper is as follows: Section II gives the details on the ice blockage estimation approach, Section III presents case study results using eleven years of recorded data, Section IV concludes this paper.

II. Problem Formulation

The proposed approach for ice blockage estimation at the water intake is outlined in Fig. 1. Recognizing that ice blockage at the water intake decreases the water flow of the conduit, the proposed approach first calculate the flow velocity coefficient of the conduit (hereafter, we call this flow velocity coefficient). The data-driven method tries to detect significant drop of the flow velocity coefficient. As shown in Fig. 1, two intake flow equations are exploited to derive the flow velocity coefficient (see Subsection D). The intake flow can be expressed from the supply and consumption perspectives (see Subsections B and C). Three detection conditions are developed to extract only significant flow velocity coefficient dips (see Subsection E-1). Three rejection conditions are also adopted to exclude false positives, i.e., improper ice

We wish to thank Matthew Carney with New York Power Authority for his valuable technical support on this project.

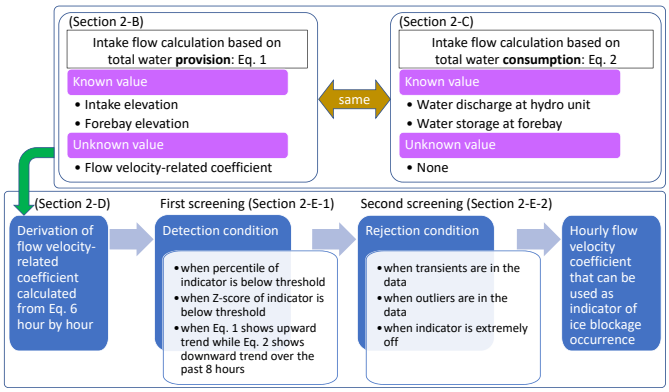

Fig. 1. Overview of proposed ice blockage estimation procedure.

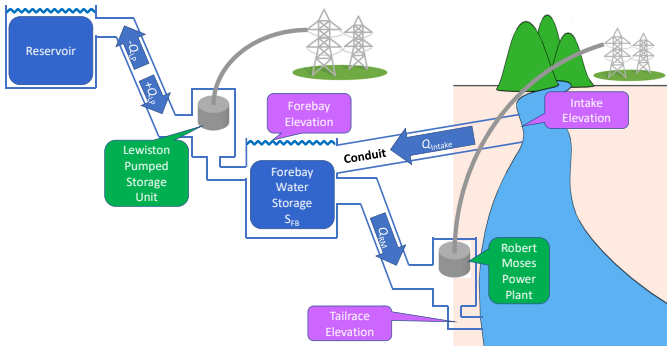

Fig. 2. Topology of NYPA hydropower facilities.

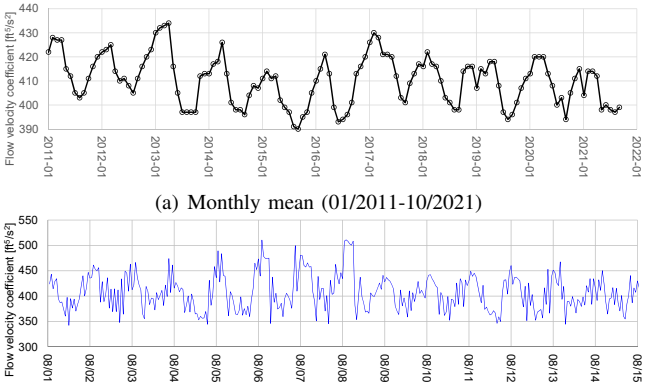

(a) Monthly mean (01/2011-10/2021)

(b) Hourly mean (08/01/2011-08/15/2011)

Fig. 3. Monthly and hourly means of flow velocity coefficient.

blockage estimation that is caused by bad data or outliers (see Subsection E-2). The remaining flow velocity coefficients passing the above conditions will serve as the indicators of the ice blockage occurrence.

This data-driven approach leverages the following recorded quantities that can be measured every minute:

- Elevation (or water level) at the intake
- Elevation at the forebay
- Water discharge at two hydropower stations (the Robert Moses and Lewiston)
- Water storage at the forebay

Note that the last two quantities in the above bullets are not directly measured, but calculated from the measured values (a detailed calculation approach is illustrated in Section II-C).

A. Relation Between Ice Blockage at Water Intake and Flow Velocity Coefficient of Conduit

The provision and consumption of the water are balanced at steady-flow conditions, i.e., before the occurrence of the ice blockage at the water intake. If the water discharge at hydropower stations is constant regardless of the occurrence of the ice blockage at the water intake, the forebay elevation is highly likely to decrease after the ice blockage event. This decrease in the water flow can be represented as the decrease in the flow velocity coefficient (smaller values express the larger friction in the conduit that thwarts smooth flows).

B. Calculation of Intake Flow from Supply Perspective

Without considering flow dynamics, the volume of water flowing into the forebay via the NPYA intake conduit can be estimated using elevations at the intake and forebay as Eq. 1:

$$Q_{\text{Intake\_s}} = 1000\sqrt{k(E_{\text{Intake}} - E_{\text{Forebay}})}[ft^3/s], \qquad (1)$$

where E_{Intake} denotes the intake elevation and E_{Forebay} denotes the forebay elevation. The coefficient, k, is constant with respect to the flow velocity coefficient of the conduit between the intake and the forebay. Eq. 1 demonstrates the intake flow from supply perspectives (Fig. 2).

As described earlier, Eq. 1 is valid at the steady-flow condition and derived based on Bernoulli's theorem. If the conduit's physical condition does not change, then the coefficient, k, should be constant. In reality, the actual steady-state coefficient fluctuates not only from season to season, but also from day to night. As shown in Fig. 3, the flow velocity coefficient, k, fluctuates by nearly $100[ft^5/s^2]$ within a day. The water discharge, $Q_{\text{Intake\_s}}$, obtained from Eq. 1, is directly leveraged as an detection condition detailed in Subsection E-1. In this paper, the coefficient, k, is set as the monthly averaged value of the previous month when using Eq. 1 to reflect the seasonal property.

C. Calculation of Intake Flow from Consumption Perspective

The water flow at the NYPA intake can also be derived from the water discharge at the Robert Moses hydropower units, the Lewiston pumped storage units, and the forebay water storage:

$$Q_{\text{Intake\_c}} = Q_{\text{RM}} - Q_{\text{LP}} + \Delta S_{\text{Forebay}}[ft^3/s], \qquad (2)$$

where Q_{RM} denotes the water discharge at the Robert Moses units, and Q_{LP} denotes the water discharge at the Lewiston pumped storage units. It is noted that the positive sign is applied when generating (e.g., $-Q_{\text{LP}}$ becomes positive when pumping). The water is stored at the forebay, expressed as S_{Forebay} (see also Fig. 2). The water storage change at the forebay is calculated from the forebay elevation:

$$\begin{aligned}\Delta S_{\text{Forebay}} &= S_{\text{Forebay}}(i) - S_{\text{Forebay}}(i-1) \\ &= 71\{E_{\text{Forebay}}(i) - E_{\text{Forebay}}(i-1)\}[ft^3/s],\end{aligned} \qquad (3)$$

where i denotes the hourly time step. The constant, 71, is specified, assuming that the shape of the forebay is represented as the cuboid.

The water discharge at the Robert Moses power station is calculated from the quartic equation, based on the rating table with respect to the active power output and gross head:

$$\begin{cases} Q_{\text{RM}} & = ax^4 + bx^3 + cx^2 + dx + e, \\ x & = 1000 P_g H^{-1.5}, \end{cases} \tag{4}$$

where P_g denotes the active power output, and H denotes the gross head. Variables, a, b, c, d, and e in Eq. 4, are coefficients, and the different sets of parameters are identified in response to three active power output bands (low, medium, and high).

The water discharge of the Lewiston pumped storage units is calculated from the cubic equation of gate reference/target or load reference (i.e., active power output reference), depending on the operating mode.

$$Q_{\text{LP}} = a'x^3 + b'x^2 + c'x + d', \tag{5}$$

where x denotes the gate position reference in pumping mode and the load reference in generating mode. Coefficients, a', b', c', and d' in Eq. 4, are individually identified in response to 36 combinations of the following three parameters:

1) Operating mode (generating, pumping)
2) Runner type (2 types)
3) Gross head (8 points with the interval of 5 feet at generating mode, 10 points with the interval of 10 feet at pumping mode)

If the current gross head is between two points, the Lewiston water discharge is calculated with the linear interpolation of the two corresponding and adjacent water discharges.

D. Flow Velocity-related Coefficient of Conduit as Ice Blockage Estimation Indicator

Equations 1 and 2 calculate the NYPA intake water flow from supply and consumption perspectives, respectively. Because values obtained from Eqs. 1 and 2 should be the same, the flow velocity-related coefficient, k, can be expressed as Eq. 6 by combining those two equations.

$$k = \frac{(Q_{\text{RM}} - Q_{\text{LP}} + \Delta S_{\text{FB}})^2}{(E_{\text{Intake}} - E_{\text{Forebay}}) \times 10^6} [ft^5/s^2]. \tag{6}$$

Strictly speaking, k is comprised of the flow velocity coefficient, conduit area, and gravity acceleration, but hereafter, we call k flow velocity coefficient. As described earlier (subsection C), Eq. 2 is less sensitive to the forebay elevation. On the other hand, Eq. 1 is highly sensitive to the forebay elevation. If water usage does not change much before and after the ice blockage at the water intake, then the forebay elevation, E_{Forebay} could decrease significantly. This results in:

- Smaller numerator due to smaller ΔS_{FB} (see Eq. 3),
- The larger denominator of Eq. 6,

which decreases k, i.e., it leads to the smaller k.

E. Ice Blockage Indicator Detection Condition

1) Statistic-oriented Condition: Although the ice blockage is likely to happen when the flow velocity coefficient decreases drastically, a fixed scalar threshold cannot be leveraged due to the time-varying flow velocity coefficient (see Fig. 3). A fixed percentile does not always work as the threshold because the frequency of the significant decrease in the flow velocity coefficient is also quite different between summer and winter. Furthermore, checking whether the z-score of the flow velocity coefficient exceeds 2σ or 3σ range is not always valid because the distribution of the flow velocity coefficient (or the peak-to-peak of the coefficient fluctuation) would be different between summer and winter.

Therefore, we propose to adopt two anomaly indicators as the dynamic thresholds (i.e., monthly updating thresholds):

- Percentile of the flow velocity coefficient: smaller than 0.5%,
- Magnitude of standard deviation of the flow velocity coefficient: smaller than -2.5σ.

2) Intake Flow Gradient-based Condition: Reference [4] provides the following new findings:

- The water flow decrease emerges a few hours (typically 1.5-3 hours) after the forebay elevation decrease,
- The ice blockage mostly continues over 8 hours.

The first finding indicates that Eq. 1 increases at least for two hours along with the decrease in forebay elevation decrease. During that time, Eq. 2 must show a downward trend. This feature may be projected into the following necessary conditions of the ice blockage occurrence.

$$\begin{cases} Q_{\text{Intake\_s}}(i) > Q_{\text{Intake\_s}}(i-1) \\ Q_{\text{Intake\_s}}(i-1) > Q_{\text{Intake\_s}}(i-2) \\ Q_{\text{Intake\_c}}(i) < Q_{\text{Intake\_c}}(i-1) \\ Q_{\text{Intake\_c}}(i) < Q_{\text{Intake\_c}}(i-2) \end{cases} \tag{7}$$

The above signature displays only at the beginning of the ice blockage event, and the significant drop of the flow velocity coefficient occurs a few hours after that signature. Therefore, the off delay timer of 8 hours is applied for Eq. 7, referring to the second finding in [4]. The set of inequality conditions and Eq. 7 with 8 hours of the off delay timer significantly contribute to reducing false positives in summertime (see Section III).

In addition to the above detection (or adoption) conditions, $Q_{\text{Intake\_s}}(i) < Q_{\text{Intake\_s}}(i+1)$ is applied only at the timing when k satisfies these conditions to ensure that the intake water flow from $Q_{\text{Intake\_s}}$ surely turns over and decreases. The structure of detection conditions is illustrated in Fig. 4.

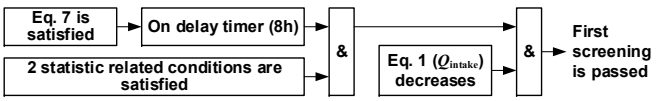

Fig. 4. Logic flow of detection condition in first screening.

F. Ice Blockage Indicator Rejection Condition

The ice blockage estimation indicator is not always reliable, and its performance is often deteriorated due to the following reasons:

- Transients or spikes in the measured data,
- Outliers in the measured data.

1) Transients: Spikes (similar to impulse response) are detected using the second-order derivatives of relevant quantities (E_{Forebay}, Q_{RM}, Q_{LP}, and $\Delta S_{\text{Forebay}}$). Transients (significant immediate changes) are detected using the first-order derivative of the following variables; E_{Forebay} and $\Delta S_{\text{Forebay}}$. When these derivatives are lower than the 2nd percentile or greater than the 98th percentile, they are treated as transient or spike (both negative and positive directions).

2) Outlier: The outlier may be identified with the historical data and their probabilities. The NYPA has accumulated historical data since 2008 and found the following stats:

- 0.1 percentile of the forebay water level: 536.6 ft,
- 99.9 percentile of the forebay water level: 561.2 ft,
- 0.1 percentile of the intake water level: 560.2 ft,
- 99.9 percentile of the intake water level: 562.4 ft.

As shown from the above bullets, the forebay elevation is quite unlikely to be equal to or higher than 561.2 ft, and the intake elevation is highly unlikely to be lower than 560.2 ft. Considering the margin of the intake elevation, 559 ft is chosen as the threshold that detects the outlier of the intake elevation. On the other hand, no margin is considered for the threshold of the forebay elevation, because the 99.9 percentile of the forebay elevation is already within the likely range of the intake elevation. Besides, an extreme value of k is also treated as invalid. The rejection conditions due to outliers are:

$$E_{\text{Intake}} < 559 \text{ ft}, \; E_{\text{Forebay}} > 561 \text{ ft}, \; \frac{\Sigma_{i=1}^{744} k(i) - k(i)}{\sigma_k} < -4.0.$$

III. Verification of the Proposed Ice Blockage Detection Approach

According to [2], [4], historical ice blockage events only occurred in Dec., Jan., Feb., and Mar. Therefore, the proposed indicator's performance is examined in Jan., Feb., and Mar. and we report three representative detected events. Operational logs that Niagara River Control Center generated are leveraged for the collateral evidence of the possible ice blockage events.

A. Recorded Data and Estimated Ice Blockage Occurrences

The recorded data are originally minute-to-minute data and cover from Jan. 2011 to Oct. 2021. Water level data are averaged and converted to hourly data, while water flow data are summed up hour by hour to generate hourly data. When no data shares over 50% of the hourly data (i.e., longer than 30 minutes in total), the NaN data is assigned. The ice blockage occurrence has been estimated three times over the past 11 years (03/05/2015, 01/07/2018, 02/11/2019).

B. First Ice Blockage Event (03/05/2015)

The operational log reported that the shore ice (frazil ice) had been intermittently recognized by system operators since 03/03/2015 and continuously observed since 03/04/2015. Specifically, the shore ice had been scattered (and likely to be obstructed) at the water intake since noon on 03/04/2015 (until the ice blockage occurrence). Figure 5 indicates that the intake water flow obtained from Eq. 1 increased on 03/05/2015 from 3-7 AM, and the intake water flow obtained from Eq. 2 decreased from 4-10 AM on the same day. Then, the flow velocity coefficient significantly dropped, and the ice blockage event was detected at 8 AM.

C. Second Ice Blockage Event (01/07/2018)

The operational log states that the *anchor ice* had been observed by system operators on 01/07/2018 from 1-7 PM. The *anchor ice* was also observed on the other side of the river during the same time. Figure 6 indicates that the intake water flow obtained from Eq. 1 increased on 01/07/2018 from 5-7 PM, and the intake water flow obtained from Eq. 2 decreased from 5-8 PM on the same day. Then, the flow velocity coefficient significantly dropped, and the ice blockage flag was on at 8 PM.

D. Third Ice Blockage Event (02/11/2019)

According to the operational log, the shore ice (frazil ice) had been intermittently recognized by the system operator since 02/10/2019. Besides, the lake ice had been observed before observing the shore ice at the NYPA intake (i.e., 02/09/2019). The lake ice had also been seen on the other side of the river when the shore ice had been placed at the NYPA intake (since 02/11/2019 at 3 PM). Figure 7 indicates that the intake water flow obtained from Eq. 1 increased on 02/11/2019 from 7-10 PM, and the intake water flow obtained from Eq. 2 decreased from 8 PM - 12 AM on the same day. Then, the flow velocity coefficient significantly dropped, and the ice blockage occurrence was estimated on 02/12/2019 at 3

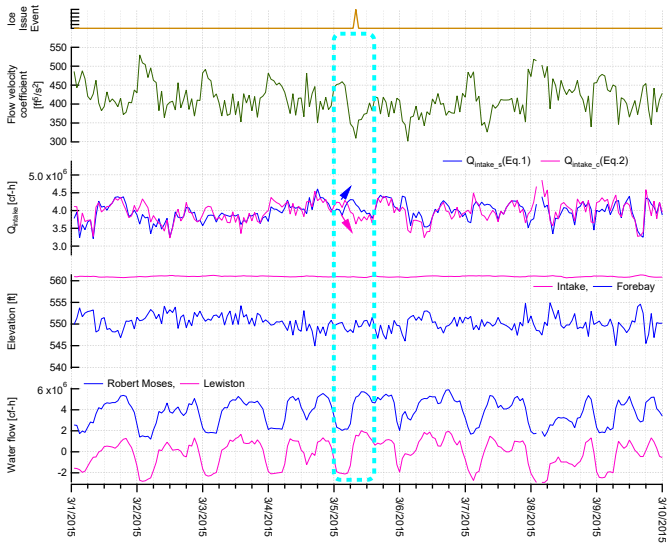

Fig. 5. The estimated ice blockage occurrence in Mar. 2015.

TABLE I
MONTHLY FREQUENCY OF ICE BLOCKAGE (HOUR BY HOUR, 2011-2021)

	Frequency of ice blockage													
	Jan.	Feb.	Mar.	Apr.	May.	Jun.	Jul.	Aug.	Sep.	Oct.	Nov.	Dec.	Dec.-Mar.	Annual
No percentile-based threshold	3	2	1	0	1	0	0	1	0	0	0	0	6	8
No z-score-based threshold	1	2	1	0	1	1	1	1	0	0	0	0	4	8
No outlier-based rejection	1	1	1	0	1	1	0	0	0	0	0	0	3	5
No transients-based rejection	3	5	1	0	2	0	1	0	0	0	0	0	9	12
Q_{intake} gradient based on Eq. 7	1	4	1	3	3	1	2	1	1	4	3	0	6	24
All conditions leveraged	1	1	1	0	1	0	0	0	0	0	0	0	3	4

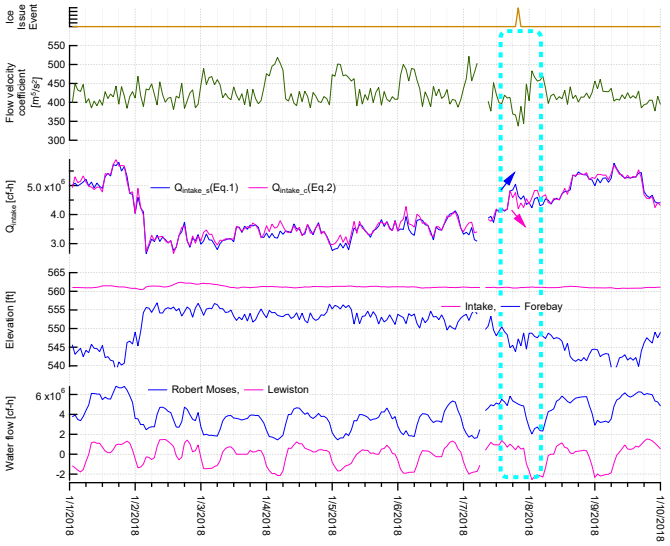

Fig. 6. The estimated ice blockage occurrence in Jan. 2018.

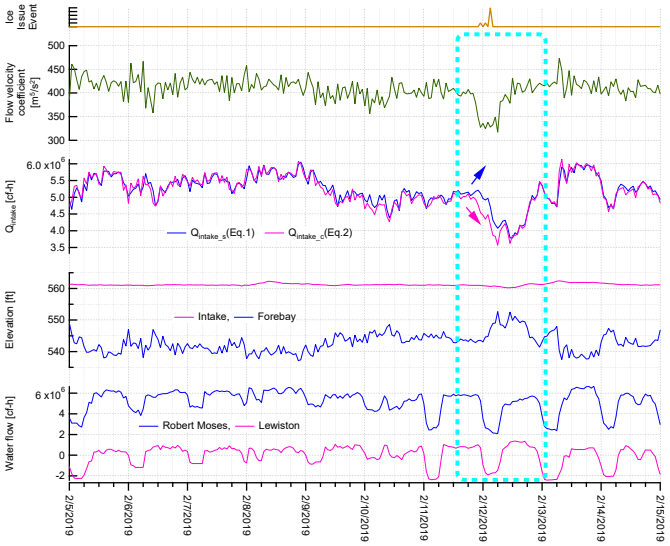

Fig. 7. The estimated ice blockage occurrence in Feb. 2019.

AM. The significant decrease in the flow velocity coefficient continued for over 6 hours on Feb. 11 - Feb. 12.

E. Verification of Screening Function

Each detection and rejection condition in Fig. 1 is deactivated one by one to clarify how each condition eliminates false positives (Tab. I). The last column from the right in Tab. I shows the frequency of the estimated ice blockage occurrence throughout the year, while the second to the last column in Tab. I shows the frequency of the occurrence in the winter season only. Table I indicates that the transients-based rejection condition drastically eliminates false positives in wintertime, while the water intake gradient condition based on Eq. 7 notably removes false positives in the summertime.

IV. CONCLUSION

This paper proposed an index that estimates the ice blockage at the water intake using the estimated flow velocity coefficient of the conduit. Acceptance and rejection conditions were also created to combat false positives. The performance of the proposed ice blockage event detection algorithm was verified with 11 years of recorded data at Niagara hydropower stations. The proposed indicator detected three possible ice blockage events. The operator's log states that the anchor ice, lake ice, or shore ice was continuously observed several hours before detecting the three ice blockage event. Although this evidence demonstrates the usefulness of the proposed ice blockage event detection algorithm, the event detection performance can be further improved with a more sophisticated dynamic model of the conduit. The installation of underwater cameras or sonar devices in the future will help fully validate the proposed ice blockage detection algorithm for the water intake infrasture.

REFERENCES

[1] S. F. Daly, "Frazil ice blockage of intake trash racks," US Army Corps of Engineers, Cold Regions Technical Digest, Tech. Rep. 91-1, Mar. 1991.

[2] S. F. Day and R. Ettema, "Frazil ice blockage of water intakes in the great lakes," *Journal of Hydraulic Engineering*, vol. 132, no. 8, pp. 814–824, Aug. 2006.

[3] K. L. Carey, "Ice blockage of water intakes," Cold Regions Research and Engineering Lab, Tech. Rep. PB-294319, Mar. 1979.

[4] M. Richard and B. Morse, "Multiple frazil ice blockages at a water intake in the st. lawrence river," *Cold Regions Science and Technology*, vol. 53, pp. 131–149, 2008.

[5] T. Ghobrial, A. Pierre, and B. Morse, "Field measurements of frazil ice accumulation at a water intake on the mille-iles river quebec," in *CGU HS Committee on River Ice Processes and the Environment 21st Workshop on the Hydraulics of Ice Covered Rivers*, Canada, Aug.-Sep. 2021, pp. 1–17.

[6] G. P. Williams, "Frazil ice: A review of its properties with a selected bibliography," *Eng. J. (Can.)*, vol. 42, no. 11, pp. 55–60, Dec. 1959.

[7] S. Q. Ye and J. C. Doering, "Simulation of the supercooling process and frazil evolution in turbulent flows," *Can. J. Civ. Eng.*, vol. 31, no. 6, pp. 915–926, Dec. 2004.

[8] S. F. Daly, "Frazil ice dynamics," Cold Regions Research and Engineering Lab, Tech. Rep. Monograph 84-1, Apr. 1984.

[9] N. E. Yankielun and J. J. Gagnon, "Laboratory tests of a time- domain reflectometry system for frazil ice detection," *Can. J. Civ. Eng.*, vol. 26, no. 2, pp. 168–176, Apr. 1999.

[10] T. H. Logan, "Prevention of frazil ice clogging of water intakes by application of heat," Engineering and Research Center Bureau of Reclamation, Tech. Rep. REC-ERC-74-15, Apr. 1974.